Improved digital backward propagation for the compensation of inter-channel nonlinear effects in polarization-multiplexed WDM systems

Eduardo F. Mateo,[1,*] Xiang Zhou,[2] and Guifang Li[1]

[1]*CREOL, The College of Optics and Photonics, University of Central Florida, 4000 Central Florida Blvd., Orlando, FL, 32816, USA*

[2]*AT&T Labs – Research, 200 Laurel Avenue South, Middletown, NJ, 07748, USA*

**emateo@creol.ucf.edu*

Abstract: An improved split-step method (SSM) for digital backward propagation (DBP) applicable to wavelength-division multiplexed (WDM) transmission with polarization-division multiplexing (PDM) is presented. A coupled system of nonlinear partial differential equations, derived from the Manakov equations, is used for DBP. The above system enables the implementation of DBP on a channel-by-channel basis, where only the effect of phase-mismatched four-wave mixing (FWM) is neglected. A novel formulation of the SSM for PDM-WDM systems is presented where new terms are included in the nonlinear step to account for inter-polarization mixing effects. In addition, the effect of inter-channel walk-off is included. This substantially reduces the computational load compared to the conventional SSM.

OCIS codes: (060.2330) Fiber optics communications; (060.1660) Coherent communications; (190.4370) Nonlinear optics, fibers.

References and links

1. P. P. Mitra, and J. B. Stark, "Nonlinear limits to the information capacity of optical fibre communications," Nature **411**(6841), 1027–1030 (2001).
2. M. G. Taylor, "Coherent Detection Method using DSP for Demodulation of Signal and Subsequent Equalization of Propagation Impairments," IEEE Photon. Technol. Lett. **16**(2), 674–676 (2004).
3. X. Liu and D. A. Fishman, "A Fast and Reliable Algorithm for Electronic Pre-Equalization of SPM and Chromatic Dispersion," in OFC, (Optical Society of America, 2006), paper OThD4.
4. E. Yamazaki, F. Inuzuka, K. Yonenaga, A. Takada, and M. Koga, "Compensation of interchannel crosstalk induced by optical fiber nonlinearity in carrier phase-locked WDM system," IEEE Photon. Technol. Lett. **19**(1), 9–11 (2007).
5. X. Li, X. Chen, G. Goldfarb, E. Mateo, I. Kim, F. Yaman, and G. Li, "Electronic post-compensation of WDM transmission impairments using coherent detection and digital signal processing," Opt. Express **16**(2), 880–888 (2008).
6. E. Ip, and J. M. Kahn, "Compensation of Dispersion and Nonlinear Impairments Using Digital Backpropagation," J. Lightwave Technol. **26**(20), 3416–3425 (2008).
7. G. Goldfarb, M. G. Taylor, and G. Li, "Experimental Demonstration of Fiber Impairment Compensation Using the Split-Step Finite-Impulse-Response Filtering Method," IEEE Photon. Technol. Lett. **20**(22), 1887–1889 (2008).
8. F. Zhang, Y. Gao, Y. Luo, J. Li, L. Zhu, L. Li, Z. Chen, and A. Xu, "Experimental Demonstration of Intra-channel Nonlinearity Mitigation in Coherent QPSK Systems with Nonlinear Electrical Equalizer," Electron. Lett. **46**(5), 353–355 (2010).
9. R. Waegemans, S. Herbst, L. Holbein, P. Watts, P. Bayvel, C. Fürst, and R. I. Killey, "10.7 Gb/s electronic predistortion transmitter using commercial FPGAs and D/A converters implementing real-time DSP for chromatic dispersion and SPM compensation," Opt. Express **17**(10), 8630–8640 (2009).
10. X. Liu, F. Buchali, and R. W. Tkach, "Improving the Nonlinear Tolerance of Polarization-Division-Multiplexed CO-OFDM in Long-Haul Fiber Transmission," J. Lightwave Technol. **27**(16), 3632–3640 (2009).
11. F. Yaman and G. Li, "Nonlinear Impairment Compensation for Polarization-Division Multiplexed WDM Transmission Using Digital Backward Propagation," IEEE Photonics J. **1**(2), 144–152 (2009).

#137629 - $15.00 USD Received 3 Nov 2010; revised 1 Dec 2010; accepted 10 Dec 2010; published 4 Jan 2011

12. E. Ip, "Nonlinear Compensation Using Backpropagation for Polarization-Multiplexed Transmission," J. Lightwave Technol. **28**(6), 939–951 (2010).
13. E. F. Mateo, F. Yaman, and G. Li, "Efficient compensation of inter-channel nonlinear effects via digital backward propagation in WDM optical transmission," Opt. Express **18**(14), 15144–15154 (2010).
14. G. P. Agrawal, *Nonlinear fiber optics*, (Academic Press, 2007).
15. O. Sinkin, R. Holzlohner, J. Zweck, and C. R. Menyuk, "Optimization of the split-step Fourier method in modeling optical-fiber communications systems," J. Lightwave Technol. **21**(1), 61–68 (2003).
16. E. F. Mateo, and G. Li, "Compensation of interchannel nonlinearities using enhanced coupled equations for digital backward propagation," Appl. Opt. **48**(25), F6–F10 (2009).
17. E. F. Mateo, L. Zhu, and G. Li, "Impact of XPM and FWM on the digital implementation of impairment compensation for WDM transmission using backward propagation," Opt. Express **16**(20), 16124–16137 (2008).
18. P. Poggiolini, A. Carena, V. Curri, and F. Forghieri, "Evaluation of the computational effort for chromatic dispersion compensation in coherent optical PM-OFDM and PM-QAM systems," Opt. Express **17**(3), 1385–1403 (2009).
19. V. Oppenheim, and R. V. Schafer, *Digital Signal Processing*, (Prentice-Hall, 1975).
20. J. G. Proakis, *Digital Communications*, (McGraw-Hill, 2001).

1. Introduction

There has been and continues to be much research on high data-rate and spectrally-efficient fiber communication systems. Higher bit-rates per channel involve the deployment of high-order modulation formats, requiring increased SNR and hence higher power per channel. Alternatively, higher spectral efficiency also demands tightly spaced wavelength-division multiplexed (WDM) channels to optimize the operational bandwidth of optical amplifiers. Together with WDM, polarization-division multiplexing (PDM) is also deployed to double the spectral efficiency. The above scenario clearly leads to increased nonlinearity in the form of intra- and inter-channel effects as well as inter-polarization effects. Therefore, the mitigation or compensation of fiber impairments which involve Kerr nonlinearity and PDM becomes crucial to increasing transmission capacity [1].

Recently, digital backward propagation (DBP) has been proposed for the *comprehensive* compensation of fiber impairments. DBP is based first, on the coherent detection of the optical signal [2] and second, on the implementation of backward propagation in the digital domain. This implementation consists on solving the z-reversed propagation equations that describe nonlinear transmission in fibers. Provided that the channel characteristics are known, and provided the WDM channels share the same optical path, any deterministic effect can be pre/post-compensated at the transmitter/receiver. The joint compensation of dispersion and nonlinearity allows increasing the launch power to values beyond the traditional nonlinear limit. Therefore, higher OSNR is achieved and transmission reach can be extended.

In single polarization systems, pre- and post- compensation via DBP were first proposed in [3–6]. Experimental demonstration of DBP in multi-channel systems was reported in [7] and single channel experiments were carried out in [8,9]. DBP in PDM systems using vectorial backward propagation has been reported in [10] for single channel and in [11,12] for WDM.

Despite its proven efficacy in both improving performance and extending reach, DBP is still challenging in terms of DSP complexity and therefore, it is still far from being deployed in current systems. Recently, an advanced split-step method (SSM) was presented in [13] to reduce the computational load of single-polarization DBP. In [13], the compensation of single-polarization inter-channel effects via DBP was shown to increase the transmission reach from 800 to 2000 km. Moreover, the computational load can be reduced by more than a factor of 4 with respect to the conventional SSM.

In this paper, an advanced SSM method is presented for PDM systems. Several aspects are different in the PDM case compared to the single-polarization case studied in [13]. First, a new coupled system of nonlinear partial differential equations is derived for the backward propagation of PDM signals. Such system is obtained from the Manakov equations, instead of the scalar nonlinear Schrodinger equation, which can be used to describe vectorial nonlinear propagation in fiber with randomly varying birefringence [14]. In contrast to the scalar case,

#137629 - $15.00 USD Received 3 Nov 2010; revised 1 Dec 2010; accepted 10 Dec 2010; published 4 Jan 2011

the coupled system of equations for PDM includes non-conservative terms in the form of phase-matched interaction between the modulated polarization tributaries. When such non-conservative terms are consider in DBP, a new solution (with no counterpart in the single-polarization case) has to be obtained for the nonlinear step of the SSM. In this paper, we propose a quasi-analytical solution for the computation of the non-conservative contribution. In addition, the advanced SSM presented in [13] is applied to the PDM case. Here, a walk-off factorization is applied to reduce the computation complexity of the SSM. Such advanced-SSM is now extended for the PDM and the factorization of the walk-off is also applied to the PDM non-conservative terms. From a performance point of view, the impact of the PDM phase-matched non-conservative terms is analyzed, for the first time to our knowledge, in the context of digital backward propagation.

2. Digital backward propagation for PDM-WDM systems

In a PDM-WDM system with coherent detection, the full reconstruction of the vector optical field can be achieved by using a polarization- and phase-diverse receiver. The reconstructed field will be used as the input for DBP in order to compensate the transmission impairments. Let $E_{xm}(t,z)$ and $E_{ym}(t,z)$ be the polarization tributaries of the complex received field for the mth-channel where $m=\{1,2,\ldots,N\}$ and N is the number of channels. The reconstructed total optical field is given by: $\mathbf{E}=\mathbf{x}E_x+\mathbf{y}E_y$, where $E_{(x,y)}=\sum_m \hat{E}_{(x,y)m}\exp(im\Delta\omega t)$ and $\Delta f=\Delta\omega/2\pi$ is the channel spacing.

In general, optical communication fibers exhibit residual birefringence responsible for the random scattering of the state of polarization over a length scale of 10 - 100 m [14]. Moreover, the typical power values used in communication systems lead to rather long nonlinear lengths. Along the nonlinear length, the state of polarization changes fast and randomly, and the effect of the local state of polarization on the overall nonlinear interaction can be averaged over the entire Poincaré sphere. As a consequence of the above, the vector optical propagation can be described by the so-called Manakov system [11,14], which is expressed as follows for backward propagation:

$$-\frac{\partial E_{(x,y)}}{\partial z}+\frac{\alpha}{2}E_{(x,y)}+\frac{i\beta_2}{2}\frac{\partial^2 E_{(x,y)}}{\partial t^2}+-\frac{\beta_3}{6}\frac{\partial^3 E_{(x,y)}}{\partial t^3}+i\frac{8}{9}\gamma\left(\left|E_{(x,y)}\right|^2+\left|E_{(y,x)}\right|^2\right)E_{(x,y)}=0, \quad (1)$$

where β_j represents the jth-order dispersion, α is the absorption coefficient, γ is the nonlinear parameter and t is the retarded time frame. The above system includes both coherent (FWM) and incoherent (SPM, XPM) nonlinear effects between channels and polarization components. As explained in [16], the coherent nature of FWM requires: i) the full reconstruction of the entire WDM band, ii) enough up-sampling to avoid aliasing of newly generated FWM products, iii) very short step sizes and iv) phase-locked local oscillators to preserve the relative phase between channels.

Alternatively, inter-channel coherent terms can be omitted in backward propagation by introducing the field expressions $E_{(x,y)}=\sum_m \hat{E}_{(x,y)m}\exp(im\Delta\omega t)$ into Eq. (1), expanding the $\left|E_{(x,y)}\right|^2$ terms and ignoring phase-mismatched terms. This leads to the following coupled equations,

$$\begin{aligned}-\frac{\partial \hat{E}_{xm}}{\partial z}+\left(\frac{\alpha}{2}+L_m+iC_{xm}\right)\hat{E}_{xm}+iK_m\hat{E}_{ym}=0,\\ -\frac{\partial \hat{E}_{ym}}{\partial z}+\left(\frac{\alpha}{2}+L_m+iC_{ym}\right)\hat{E}_{ym}+iK_m^*\hat{E}_{xm}=0,\end{aligned} \quad (2)$$

#137629 - $15.00 USD Received 3 Nov 2010; revised 1 Dec 2010; accepted 10 Dec 2010; published 4 Jan 2011

where L_m, $C_{(x,y)m}$ and K_m represent the linear dispersive operator, the phase-insensitive XPM contribution and a polarization mixing (PolM) term, respectively, given by:

$$L_m = D_{1m}\frac{\partial}{\partial t} + D_{2m}\frac{\partial^2}{\partial t^2} + D_{3m}\frac{\partial^3}{\partial t^3}, \tag{3}$$

$$C_{(x,y)m} = -\frac{8}{9}\gamma\left(P_{xm} + P_{ym} + \sum_{\forall q\neq m} R_{(x,y)q}\right) \tag{4}$$

$$K_m = -\frac{8}{9}\gamma\left(\sum_{\forall q\neq m} \hat{E}^*_{yq}\hat{E}_{xq}\right), \tag{5}$$

where, $P_{(x,y)m} = \left|\hat{E}_{(x,y)m}\right|^2$ and $R_{(x,y)m} = 2P_{(x,y)m} + P_{(y,x)m}$. Clearly, the first two terms on the right hand side of Eq. (4) represent the SPM contribution whereas $R_{(x,y)m}$ includes the XPM contribution. The dispersion parameters are given by: $D_{1m} = m\beta_2\Delta\omega - m^2\beta_3\Delta\omega^2/2$, $D_{2m} = i\beta_2/2 - m\beta_3\Delta\omega/2$ and $D_{3m} = -\beta_3/6$. Equations (2) neglect any interaction where the relative phase between the WDM channels is relevant. Moreover, when the PolM term K_m is included, the relative phase between the polarization components of each channel is relevant. Therefore, the relative phase of the polarization tributaries has to be preserved at the receiver. This condition is typically fulfilled in polarization diverse receivers, where each local oscillator is split into orthogonal components to receive the PDM tributaries of each channel.

The above system of equations is solved in the digital domain by the well-known Split-Step Method (SSM) [14–16]. This method relies on decoupling the linear and nonlinear contributions in Eq. (2) over a sufficiently short distance. In order for this method to be accurate, the step size has to be short enough to ensure: (i) The solution of the linear part from z to $z+h$ is not perturbed by the variations of the optical fields due to nonlinear effects and (ii) The solution of the nonlinear part from z to $z+h$ is not perturbed by the variations of the optical fields due to linear effects. Under these conditions, the step size will be limited by the fastest of the above variations.

Typically, the linear step is solved in the frequency domain using efficient algorithms for both the direct and inverse Fourier Transforms.

$$\hat{E}_{(x,y)m}(t, z+h) = F^{-1}\left\{F\left[\hat{E}_{(x,y)m}(t,z)\right]H_m(\omega,h)\right\}, \tag{6}$$

with the following multi-channel linear transfer function,

$$H_m(\omega,h) = \exp\left[\left(i\beta_2\frac{(\omega-m\Delta\omega)^2}{2} + i\beta_3\frac{(\omega-m\Delta\omega)^3}{6}\right)h\right] \tag{7}$$

The above approximation is valid provided that the spectral change induced by nonlinearity is weak over the step length. Fourier domain filtering requires block-by-block computation which can be efficiently implemented by the overlap-and-add or the overlap-and-save methods [18,19].

For the nonlinear step, the linear term L_m is neglected. By transforming the optical envelopes as follows, $E_{(x,x)m} = \hat{E}_{(x,x)m}\exp(\alpha z/2)$, Eq. (2) become,

#137629 - $15.00 USD Received 3 Nov 2010; revised 1 Dec 2010; accepted 10 Dec 2010; published 4 Jan 2011

$$
\begin{aligned}
-\frac{\partial E_{xm}}{\partial z} + iC_{xm}e^{\alpha z}E_{xm} + iK_m e^{\alpha z}E_{ym} = 0,\\
-\frac{\partial E_{ym}}{\partial z} + iC_{ym}e^{\alpha z}E_{ym} + iK_m^* e^{\alpha z}E_{xm} = 0,
\end{aligned}
\tag{8}
$$

The above system lacks a closed-form solution due to the coupling term K_m. This is a FWM-like term which provides energy transfer between channels and polarization components. To solve the above system, a multi-step approach will be used. First, by neglecting the coupling term K_m, Eq. (8) have the following solution,

$$
E_{(x,y)m} = E_{(x,y)m0}\exp\left(i\int_z^{z+h} C_{(x,y)m}e^{\alpha z'}dz'\right). \tag{9}
$$

In a second step, the terms $C_{(x,y)m}$ are neglected in Eqs. (8). By taking the average of the coupling terms,

$$
\eta_m = \frac{1}{z}\int K_m e^{\alpha z'}dz', \tag{10}
$$

Equations (8) become,

$$
\begin{aligned}
-\frac{\partial E_{xm}}{\partial z} + i\eta_m E_{ym} = 0,\\
-\frac{\partial E_{ym}}{\partial z} + i\eta_m^* E_{xm} = 0,
\end{aligned}
\tag{11}
$$

By taking derivates, the above system can be decoupled and it has the following general solution,

$$
E_{(x,y)m} = a_{(x,y)}e^{i|\eta_m|z} + b_{(x,y)}e^{-i|\eta_m|z}, \tag{12}
$$

where $a_{(x,y)}$ and $b_{(x,y)}$ are integration constants. By applying initial conditions, Eq. (12) can be rewritten as,

$$
\begin{aligned}
E_{xm} = E_{xm0}\cos\left(|\eta_m|z\right) - iE_{ym0}\frac{\eta_m}{|\eta_m|}\sin\left(|\eta_m|z\right),\\
E_{ym} = E_{ym0}\cos\left(|\eta_m|z\right) - iE_{xm0}\frac{\eta_m^*}{|\eta_m|}\sin\left(|\eta_m|z\right),
\end{aligned}
\tag{13}
$$

Finally, by proceeding in a similar way as with the SSM, we can group Eq. (9) and Eq. (13) as follows,

$$
\begin{aligned}
E_{xm}(t,z+h) = E_{xm}(t,z)e^{i\phi_{xm}}\cos\left(|Q_m|\right) - iE_{ym}(t,z)e^{i\phi_{ym}}Q_m\,\mathrm{sinc}\left(|Q_m|\right),\\
E_{ym}(t,z+h) = E_{ym}(t,z)e^{i\phi_{ym}}\cos\left(|Q_m|\right) - iE_{xm}(t,z)e^{i\phi_{xm}}Q_m^*\,\mathrm{sinc}\left(|Q_m|\right),
\end{aligned}
\tag{14}
$$

where,

$$
\phi_{(x,y)m} = \int_z^{z+h} C_{(x,y)m}e^{\alpha z'}dz', \tag{15}
$$

$$
Q_m = \int_z^{z+h} K_m e^{\alpha z'}dz'. \tag{16}
$$

In the conventional split-step method, the integrals in Eqs. (15-16) are approximated by,

#137629 - $15.00 USD Received 3 Nov 2010; revised 1 Dec 2010; accepted 10 Dec 2010; published 4 Jan 2011

$$\phi_{(x,y)m}(t,z+h) = h_{eff} C_{(x,y)m}(t,z), \tag{17}$$

$$Q_m(t,z+h) = h_{eff} K_m(t,z), \tag{18}$$

where $h_{eff} = [\exp(\alpha h) - 1]/\alpha$ is the effective step size. In general, within the split-step formalism, the above approximations are valid provided the functions $C_{(x,y)m}$ and K_m are not significantly modified due to dispersion along the step size. Dispersion plays a dual role in modifying the waveforms. On the one hand, it creates intra-channel pulse broadening at a length scale given by $L_D = \left(|\beta_2| B^2\right)^{-1}$. This pulse broadening is intrinsic to each channel and depends on its baud-rate, B. On the other hand, dispersion creates walk-off effect between channels. The delay between two channels m and q occurs in a length scale given by the walk-off length, $L_{wo} = \left(|\beta_2| B \Delta\omega_{mq}\right)^{-1}$ [15,17] where $\Delta\omega_{mq}$ is the frequency difference. This dual action of dispersion directly translates into the step size requirements.

Typically, the number of channels is large and $\min(L_{wo}) << L_D$ which makes walk-off the limiting effect for the step size [17]. One way to relax the step size requirements for the compensation of inter-channel effects is to separate the effects of pulse broadening and walk-off. To that end, let us rewrite Eqs. (4) and (5) by including the time delay caused by the dispersive walk-off,

$$C_{(x,y)m}(t,z) = -\frac{8}{9}\gamma\left(P_{xm}(t,z) + P_{ym}(t,z) + \sum_{\forall q \neq m} R_{(x,y)q}(t - d_{mq} z, z) \right), \tag{19}$$

$$K_m(t,z) = -\frac{8}{9}\gamma\left(\sum_{\forall q \neq m} E^*_{yq}(t - d_{mq} z, z) E_{xq}(t - d_{mq} z, z) \right), \tag{20}$$

where $d_{mq} = \beta_2(\omega_m - \omega_q)$ is the walk-off parameter between channels m and q. By Fourier transforming the above expressions, we can write,

$$C_{(x,y)m}(\omega,z) = -\frac{8}{9}\gamma\left(P_{xm}(\omega,z) + P_{ym}(\omega,z) + \sum_{\forall q \neq m} R_{(x,y)q}(\omega,z)\, \mathrm{e}^{-i d_{mq}\omega z} \right), \tag{21}$$

$$K_m(\omega,z) = -\frac{8}{9}\gamma\left(\sum_{\forall q \neq m} E^*_{yq}(\omega,z) E_{xq}(\omega,z)\, \mathrm{e}^{-i d_{mq}\omega z} \right). \tag{22}$$

Where we use the notation, $x(\omega) = \mathrm{F}\{x(t)\}$. By taking the above expressions into account, Eqs. (15) and (16) can be approximated as,

$$j_{(x,y)m}(t,z+h) = -\frac{8}{9}\gamma\left\lfloor \left(P_{xm}(t,z) + P_{ym}(t,z)\right) h_{eff} + F^{-1}\left\{ \sum_{"q \neq m} R_{(x,y)q}(\omega,z) W_{mq}(\omega,h) \right\} \right\rfloor, \tag{23}$$

$$Q_m(t,z+h) = -\frac{8}{9}\gamma\left\lfloor F^{-1}\left\{ \sum_{\forall q \neq m} \hat{E}^*_{yq}(\omega,z) \hat{E}_{xq}(\omega,z) W_{mq}(\omega,h) \right\} \right\rfloor, \tag{24}$$

where,

$$W_{mq}(\omega,h) = \frac{e^{\alpha h - i d_{mq}\omega z} - 1}{\alpha - i d_{mq}\omega}. \tag{25}$$

#137629 - $15.00 USD Received 3 Nov 2010; revised 1 Dec 2010; accepted 10 Dec 2010; published 4 Jan 2011

From a physical perspective, the filters W_{mq} can be viewed as a generalized nonlinear effective length where not only power attenuation but walk-off effects are taken into account to modify the strength of the nonlinear interaction. The walk-off factorization removes the necessity to follow the dispersive delay within the step. Therefore, the step size becomes now limited by the minimum of the nonlinear or pulse broadening lengths. In WDM systems, the nonlinear length [17] is typically shorter than the pulse broadening length. The reason is the contribution of adjacent channels to the total nonlinear phase shift.

Computationally, the above formulation requires additional direct and inverse Fourier transforms, which gives rise an increased complexity per step. However, by factorizing the walk-off effect, the step size can be substantially increased in typical WDM scenarios.

In general, the symmetric version of the split-step method must be used in order to improve the algorithm efficiency [14,15]. Here, the nonlinear phase shift is calculated by using the value of the optical field in the mid-segment. In this case a correction factor has to be added to the filter, W_{mq} [13]. By performing a change of variable in Eqs. (15-16), we can rewrite as,

$$W_{mq}(\omega,h)=\frac{e^{(\alpha-id_{mq}\omega)h}-1}{\alpha-id_{mq}\omega}e^{-(\alpha-id_{mq}\omega)h/2}$$
$$h_{eff}=\frac{e^{\alpha h}-1}{\alpha}e^{-\alpha h/2} \qquad (26)$$

Figure 1 depicts a schematic for the implementation of the split-step method, where for simplicity, the XPM module is configured by using the equivalent formulation $C_{(x,y)m}=-8\gamma\left(-P_{(x,y)m}+\sum_{\forall q}R_{(x,y)q}\right)/9$ instead of Eq. (4).

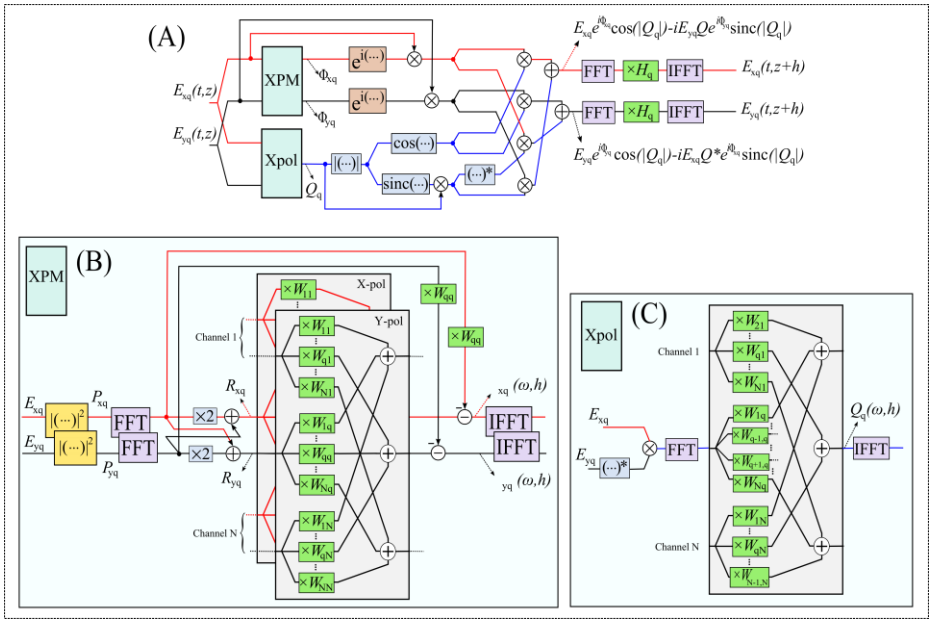

Fig. 1. (A): Block diagram for the implementation of one step using the advanced SSM..The XPM and Xpol modules are shown below. (B) Sketch of the XPM module including the filtering for walk-off factorization. For conventional SSFM, the FFT, IFFT and filters W_{mq} are removed. (C) Block of the Xpol module including the filtering for walk-off factorization. For conventional SSFM, the FFT, IFFT and filters W_{mq} are removed.

#137629 - $15.00 USD Received 3 Nov 2010; revised 1 Dec 2010; accepted 10 Dec 2010; published 4 Jan 2011

3. Simulation results and discussion

A 200 Gb/s per channel (dual polarization) 16-QAM PDM-WDM system has been simulated using the VPI TransmissionMaker. The transmission system consists of ten spans of NZ-DSF fiber with a length of 100 km per span, a dispersion parameter of $D = 4.4$ ps/km/nm and a dispersion slope of $D_s = 0.045$ ps/km/nm^2. The loss is 0.2 dB/km and the nonlinear coefficient is, $\gamma = 1.46$ /W/km. Fiber loss is compensated per span using Erbium-doped fiber amplifiers with a noise figure of 5 dB. A 24 channel WDM system with channel spacing of 50 GHz has been simulated. 16 QAM has been selected as the modulation format because it requires higher OSNRs and, hence, it can take more advantage of nonlinearity compensation techniques. The fiber is modeled as a concatenation of sections with different birefringence axes. The rate of variation of the random birefringence is modeled by using a Gaussian distribution with a variance inversely proportional to the fiber correlation length, which is assumed to be 50 m. Within each section, propagation is modeled by solving the exact nonlinear propagation equations (see Eqs. (6).1.11-12 in [14]). In our simulation, no time delay is induced between polarization components. Thus, the differential group delay between polarization modes (DGD) is equal to zero.

The entire WDM band is automatically up-sampled by VPI to properly account for third order nonlinear effects. The step-size used by VPI is chosen to keep the nonlinear phase-shift below 0.05 degrees. Raised-cosine filters are used for demultiplexing.

After forward propagation, a polarization-diverse coherent receiver is modeled as shown in Fig. 2.

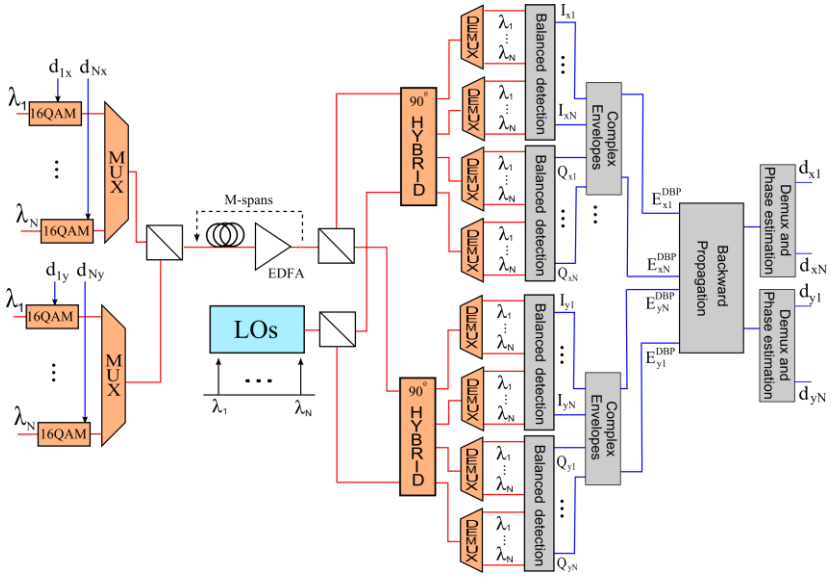

Fig. 2. Simulated TX-RX configuration with polarization diverse coherent detection.

Local oscillators, as well as transmitted lasers, are assumed to have zero linewidth. LOs frequencies are chosen to match the transmitter lasers. After detection, each polarization tributary is sampled at 2 samples/symbol and backward-propagated using Eqs. (2). After DBP, polarization demultiplexing is performed by applying the inverse Jones matrix of the system.

Then a phase estimation algorithm is performed to compensate for residual constellation rotation due to residual uncompensated nonlinearity. In this work, NZ-DSF is used because of its lower dispersion, which increases the strength of inter-channel nonlinearity with respect to SSFM. In this scenario, DBP becomes more necessary than in, for instance, systems deploying SSFM, where high local dispersion mitigates inter-channel effects more efficiently.

#137629 - $15.00 USD Received 3 Nov 2010; revised 1 Dec 2010; accepted 10 Dec 2010; published 4 Jan 2011

Five different cases will be investigated depending on the nonlinear effects included in DBP:

- DBP1: SPM compensation where the terms $R_{(x,y)m}$ and K_m are neglected. This case assumes that no information from adjacent channels is considered for DBP.
- DBP2: *Incoherent* inter-channel compensation where the term K_m is neglected. This case includes incoherent terms only; thus, the relative phase between channels and polarization components does not need to be preserved for DBP. All the transmitted channels are included for DBP.
- DBP3: *Coherent* inter-channel compensation. This case includes both incoherent inter-channel components $R_{(x,y)m}$ and the *coherent* polarization term K_m. Therefore, the relative phase between the polarization components of each individual channel has to be preserved. All the transmitted channels are included for DBP.

Finally, full compensation using Manakov system, Eq. (1), and dispersion compensation (DC) only are also performed for comparison purposes. This sets the upper and lower bounds of performance respectively. For the solution of the Manakov system, all the channels and polarizations are combined and up-sampled to form a joint band (see [16] for details). The high sampling requirements together with extremely short step sizes makes the Manakov solution impractical for an eventual DSP implementation [17]. As an estimate, in [16] it is shown that FWM compensation requires roughly 25 times more operations than XPM compensation. In this paper, PMD effects are not considered. The impact of PMD on DBP is important when the number of channels included in the XPM compensation is large. For such cases, the channels at the opposite edges cannot retain their relative orientations because of polarization-mode dispersion. For DBP to work properly these changes in the forward propagation have to be monitored and included in backward propagation. This will require dynamic monitoring of the polarization transfer matrix of the transmission fiber. With respect to the coherent polarization effects (i.e. DBP3), they are not independent of the phases of the interacting fields. Although the phase that is common to both polarizations (chromatic dispersion) at the same wavelength or common to the channels (birefringence) cancels out, the phase change coming from PMD must be accounted for the coherent polarization effects.

Figure 3 shows the baseline results after backward propagation when different effects are compensated. These results are obtained for a step size sufficiently short, from which the *Q*-factor behaves asymptotically. Values in Fig. 3 are the *Q*-factors averaged over all WDM channels. Each channel carries 1024 16-QAM symbols per polarization tributary. The *Q*-factor is obtained from the constellation by averaging the standard deviations of the 16 constellation clusters. The 16-QAM *Q*-factor calculation has been tested with direct error counting of transmission over an AWGN channel in comparison with a Gaussian model [20] which predicts the following relation between the *Q*-factor and the symbol error rate: $SER = 2 \times \mathrm{erfc}\left(10^{Q/20}\right)/3$, (e.g., a *Q*-factor of 7.6 dB for a SER of 10^{-3}).

#137629 - $15.00 USD Received 3 Nov 2010; revised 1 Dec 2010; accepted 10 Dec 2010; published 4 Jan 2011

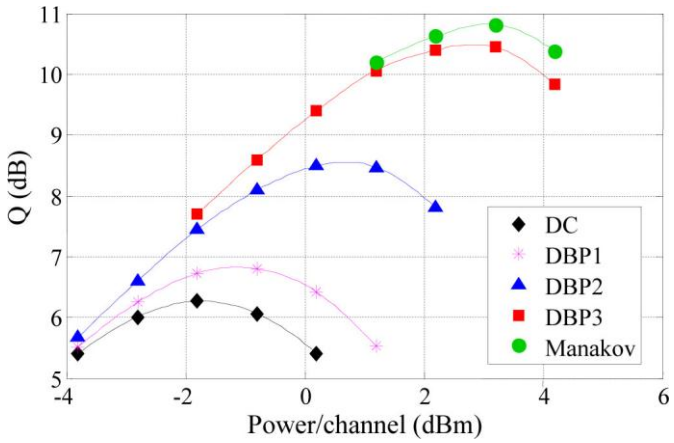

Fig. 3. DBP performance results for a PDM 16-QAM WDM system consisting of 24 channels at 200 Gb/s. DBP1 is SPM compensation. DBP2 is incoherent inter-channel compensation. DBP3 is coherent inter-channel compensation.

Several comments can be made from Fig. 3. First, SPM (DBP1) compensation provides a small improvement in terms of *Q*-factor. This is because inter-channel effects are sufficiently strong to modify the optical waveforms through forward transmission. Such modifications perturb the initial conditions for DBP making SPM compensation inefficient. With respect to DBP2, a moderate improvement of 2.1 dB is obtained with respect to dispersion compensation only. Again, the effect of the coupling term K_m in forward transmission has an impact on the initial conditions. Hence, the sole compensation of incoherent processes provides an intermediate performance. On the contrary, the compensation of both coherent and incoherent inter-channel effects (DPB3) provides a remarkable improvement of more than 4.2 dB which is close to maximum achievable performance provided by the solution of the Manakov system. The small discrepancy between DBP3 and Manakov comes from the marginal effect of FWM on the initial conditions. In this paper, a WDM system of 16QAM channels with 50 GHz spacing has been selected for simulation. From a conceptual viewpoint, DBP is a universal method in the sense that it can be applied to any modulation format provided that coherent detection is performed. However, DBP acquires more importance for high-order modulation formats since they require higher OSNR and they become, hence, more exposed to nonlinearity. With regard to channel spacing, a channel spacing that is twice the baud-rate has been chosen. Larger channel spacing would increase the walk-off between channels. This results in a more efficient averaging of the XPM effects and the performance will be increased due to weaker ASE-seeded nonlinearities [13]. Smaller channel spacing increases FWM efficiency and the difference between Manakov and DBP3 is expected to increase. Since Fig. 3 shows the Q-factor averaged over the WDM channels, it is interesting to analyze the behavior of the Q-factor for each WDM channel. Figure 4 shows such result where each DBP case is plotted at the respective optimum power. A rather homogeneous behavior is obtained for each DBP case at the optimum power. Results obtained at higher powers revealed that central channels perform worse due to a higher exposure to nonlinear interactions.

#137629 - $15.00 USD Received 3 Nov 2010; revised 1 Dec 2010; accepted 10 Dec 2010; published 4 Jan 2011

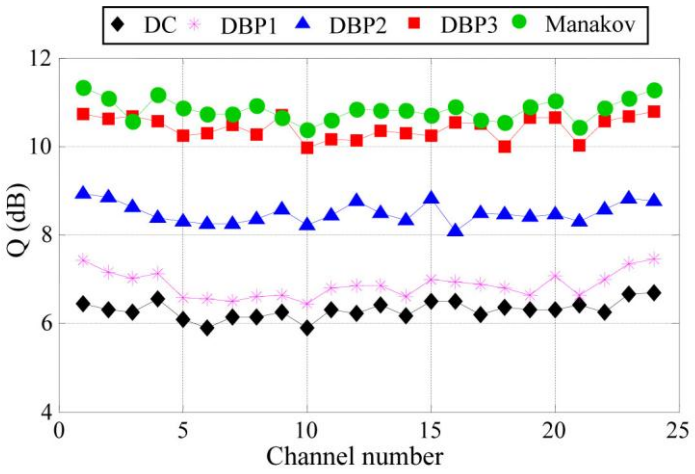

Fig. 4. Q-factor per channel for the different DBP cases. Each case is shown at the respective optimum power.

The computational efficiency of the above backward propagation schemes is now analyzed. Figure 5 shows the Q-factors as functions of the step size for the conventional and advanced SSM implementations (recall that advanced SSM stands for the walk-off factorization).

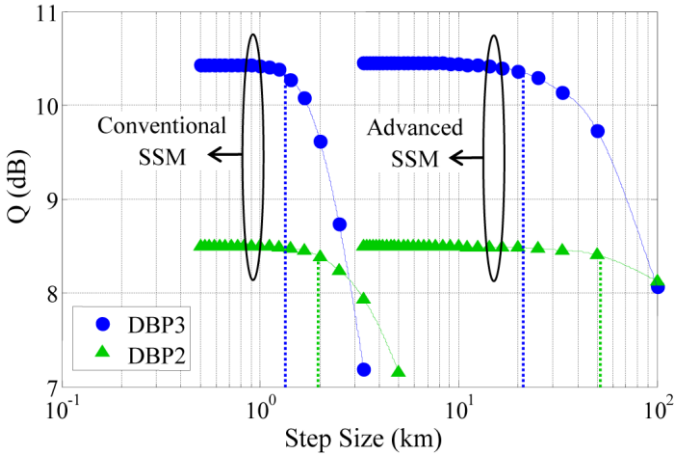

Fig. 5. *Q*-factors as functions of step size for the inter-channel compensation cases DBP2 and DBP3.

The results correspond to the respective optimum powers obtained from Fig. 3 whereas vertical markers indicate the operational (optimum) step size. This value is obtained by cubic interpolation of the simulation results and by choosing the step size value corresponding to a *Q*-value penalty of 0.1 dB with respect to the plateau value. The operational step size is chosen as a compromise between performance and computational load. The advantage of the walk-off factorization is clear in terms of step size. When comparing the advanced- and conventional-SSM, the step size is increased by a factor of 16 for the DBP3 and a factor of 26 for DBP2.

Since the dispersive walk-off imposes no restrictions on the step size for the advanced-SSM, the latter becomes limited by the nonlinear phase-shift per step, which in turn, depends on the power. This explains the difference between DBP2 and DBP3 in terms of step size when the advanced SSM is applied. The optimum operation for DBP3 happens at a power

#137629 - $15.00 USD Received 3 Nov 2010; revised 1 Dec 2010; accepted 10 Dec 2010; published 4 Jan 2011

value 3 dB higher than the one for DBP2. In addition, DBP3 includes additional nonlinear terms which also contribute to reduce the nonlinear length. The impact of the channel spacing as well as of the number of channels on the step size can be extrapolated from the results obtained in [13] for the scalar case. With respect of fiber dispersion, a different behavior can be extrapolated for the conventional and advanced algorithms. For the conventional, the step-size is proportional to the walk-off length and hence, it is reduced as the dispersion parameter of the fiber increases. Alternatively, the advanced SSFM follows the nonlinear length and it is insensitive to dispersion parameter.

Together with the step size, it is important to compare the computation requirements for each method. For simplicity only the number of complex multiplications will be considered, neglecting the number of additions. Furthermore, considerations regarding the numeric representation (fixed point/floating point) will be ignored. By recalling the schematic diagram in Fig. 1, the following number of operations is involved in backward propagation for a block-length of M samples:

- Intensity operator: M
- Filtering: $2(M+P)\log_2(M+P)+(M+P)$
- Exponential operator (4^{th} order Taylor expansion): $6M$
- Cosine operator (2^{th} order Taylor expansion): $4M$
- Sine Cardinal (3^{th} order Taylor expansion): $7M$

The number of multiplications for the exponential, cosine and sine operators is obtained by saving the square of the argument in memory [13]. These operators are sometimes implemented using look-up tables. However, look-up tables require large memory presenting a trade-off between memory and speed.

In general, the filter implementation in the frequency domain is done by the overlap-and-add method. This is done using data blocks of M samples with an additional overhead of P samples. Such overhead has to be larger than the filter length in taps [18]. Moreover FFT/IFFT algorithms operate more efficiently if $M+P$ is a power of 2. Two filter operations are implemented depending on the case, that is, walk-off filtering with $W_{mq}(\omega,h)$ and dispersion filtering with $H_m(\omega,h)$. Their respective group delays are given by,

$$\begin{aligned}\tau_W &= 2\pi\left|\beta_2\right|(N-1)\Delta f\times h,\\ \tau_H &= 2\pi\left|\beta_2\right|B\times h.\end{aligned} \tag{27}$$

By assuming a sampling rate S, the following overhead values are required for each filter operation,

$$\begin{aligned}P_W &= 2\pi\left|\beta_2\right|(N-1)\Delta f\times h\times S,\\ P_H &= 2\pi\left|\beta_2\right|B\times h\times S.\end{aligned} \tag{28}$$

By taking into account the blocks depicted in Fig. 1 the following expressions are given for the total number of multiplications per sample in the conventional SSM,

$$OP_{DBP2-c}=n_{\text{steps}}\left[4(M+P_H)\log_2(M+P_H)+2(M+P_H)+18M\right]/2M, \tag{29}$$

$$OP_{DBP3-c}=n_{\text{steps}}\left[4(M+P_H)\log_2(M+P_H)+2(M+P_H)+36M\right]/2M. \tag{30}$$

For the advanced SSM, each step involves two filter operations. For simplicity, we assume that the same overhead is used for both of them. The number of multiplications is now given by,

#137629 - $15.00 USD Received 3 Nov 2010; revised 1 Dec 2010; accepted 10 Dec 2010; published 4 Jan 2011

$$OP_{DBP2-a} = n_{\text{steps}}\left[8(M+P_W)\log_2(M+P_W)+(2N+6)(M+P_W)+16M\right]/2M, \quad (31)$$

$$OP_{DBP3-a} = n_{\text{steps}}\left[10(M+P_W)\log_2(M+P_W)+(3N+5)(M+P_W)+33M\right]/2M. \quad (32)$$

In general, the overlap-and-add method is optimized by choosing the block size that minimizes the number of multiplications. This optimum block size depends on the overhead size. In the SSM, the step size can be relatively small which causes small group delays. This eventually yields overheads of only several samples for practical sampling rates. In such scenario, the *theoretical* optimum block-size that minimizes the number of multiplications is very short. Moreover, it can be demonstrated that the block size has to be large enough to preserve numerical accuracy. Otherwise, the concatenation of steps leads to dramatic error propagation. By taking the above considerations into account, the following rules are applied to choose the block size,

1) The total block-size for filtering ($M+P$) is a power of two.

2) The minimum block size for $M+P$ is chosen to be 2^6.

3) For overhead values greater than 2^6, the total block-size ($M+P$) is chosen to minimize the number of multiplications.

By sampling at a frequency of $S=50$ GHz, Table 1 summarizes the number of operations including SPM compensation. Note that the number of operations for SPM is also given by Eq. (29) when additions are neglected.

Table 1. Summary of results for a 200 Gb/s PDM WDM system consisting in 24 channels with a 50 GHz channel spacing. Transmission is 10×100 km. Letter '-a' stands for advanced SSFM and '-c' stands for conventional SSFM.

	DC	SPM	DBP2-a	DBP2-c	DBP3-a	DBP3-c
Q-improvement	–	0.52	2.1		4.1	
h [km]	1000	100	50	1.96	20	1.35
n [steps/span]	–	1	2	51	5	74
P [samples]	44	4	106	1	42	1
M [samples]	212	60	918	63	470	63
$P+M$	2^8	2^6	2^{10}	2^6	2^9	2^6
OP [×100]	0.2	2.3	16.5	113.2	53.8	231

Table 1 shows the number of multiplications required for each method and each system. For comparison purposes, the number of operations for dispersion compensation is also shown. A factor of 4.3 in computation savings is obtained for DBP3 when the advanced SSF is used. Alternatively, a factor of 6.8 is obtained for DBP2. As explained before, this difference is due to the impact of the optimum power on the step size. Despite the increased complexity of the advanced SSM, the large step sizes allowed by the walk-off factorization substantially reduce the overall computational load.

3. Conclusion

An improved scheme for digital backward propagation (DBP) applied to PDM-WDM systems has been introduced. This new scheme is based on two new aspects. First, the backward propagation problem has been reformulated by deriving a coupled system of nonlinear partial differential equations. Such system, allows the implementation of DBP in a channel-by-channel basis by including the most relevant inter-channel and inter-polarization nonlinear terms. This formulation also allows the selective compensation of different nonlinear effects,

#137629 - $15.00 USD Received 3 Nov 2010; revised 1 Dec 2010; accepted 10 Dec 2010; published 4 Jan 2011

which has an impact on the maximum achievable Q-factor and the corresponding computational load.

Second, an improved split-step method has been used for the DSP implementation of DBP. The split-step formalism is extended to cope with new polarization-mixing terms. Likewise, the effect of dispersive walk-off is factorized by including the relative delay of the WDM channels in the computation of the nonlinear step. A 200 Gb/s PDM WDM system, consisting in 24 channels with 50 GHz channel spacing, has been simulated to assess the efficiency of the new DBP scheme. Results show that the new system of coupled nonlinear equations removes almost all the contribution of deterministic impairments. Moreover, the walk-off factorization allowed increasing the SSM step size in a substantial amount. A rigorous computation of the required number of operations showed that the improved SSM reduces the computational load by a factor of 4.3. This number is increased to almost 7 when polarization terms are not included in the backward propagation equations.

#137629 - $15.00 USD Received 3 Nov 2010; revised 1 Dec 2010; accepted 10 Dec 2010; published 4 Jan 2011